Available online at www.sciencedirect.com
ScienceDirect
Journal of Photochemistry and Photobiology A: Chemistry 192 (2007) 84–92
Journal of Photochemistry and Photobiology A:Chemistry
www.elsevier.com/locate/jphotochem

Laser photolytic approach to Cu/polymer sols and Cu/polymer nanocomposites with amorphous Cu phase

Josef Pola [a,*], Akihiko Ouchi [b,**], Snejana Bakardjieva [c], Markéta Urbanová [a], Jaroslav Boháček [c], Jan Šubrt [c]

[a] *Institute of Chemical Process Fundamentals, Academy of Sciences of the Czech Republic, 16502 Prague, Czech Republic*
[b] *National Institute of Advanced Industrial Science and Technology, AIST, Tsukuba, Ibaraki 305-8565, Japan*
[c] *Institute of Inorganic Chemistry, Academy of Sciences of the Czech Republic, 25068 Řež, Czech Republic*

Received 27 February 2007; received in revised form 3 May 2007; accepted 7 May 2007
Available online 22 May 2007

Abstract

Excimer laser photolysis of Cu(II) acetylacetonate in 2-propanol affords Cu/polymer colloidal solutions that undergo sedimentation to Cu/polymer nanocomposites. The sedimentation is little affected by O-containing surface active compounds. UV–vis and GC/MS spectral analyses of the photolysed solutions indicate that Cu/polymer colloids are formed via intermediary Cu(I) acetylacetonate decomposing into Cu nanoparticles and via simultaneous formation of a photo-polymer. Electron microscopy and X-ray diffraction analysis of the Cu/polymer nanocomposites reveal the presence of unique amorphous Cu phase.

Keywords: Cu/polymer sols; Cu/polymer nanocomposites; Laser solution photolysis; Amorphous Cu nanophase

1. Introduction

Research in nanoparticles is of great interest to scientific community due to unique physical and chemical properties and potential application of nanosystems (e.g. [1–4]). Metal nanoparticles have been prepared by a number of techniques in condensed media, where control of the size and stability of these species is more feasible than in the gas phase (e.g. [5,6]).

Nanoparticles of copper having been widely examined in recent years were produced in water by reduction [7], photolysis [8,9] and γ-radiolysis [10] of Cu(II) salts, and in organic phase by laser ablation of CuO powder [11,12], microwave-induced [13] and surfactant-catalysed [14] and phase-transfer-assisted [15,16] reduction of Cu(II) salt. Other approaches involve solvated metal atom dispersion technique [17], synthesis in microemulsions [18–20] and HRTEM-induced formation of Cu nanoparticles from simple and supramolecular complexes [21].

Conversely, Cu/polymer nanocomposites being less common materials are possibly formed by photochemical reaction in poly(*N*-vinylpyrrolidone) [8], by coating Cu nanoparticles with C/H films using a glow discharge [22] and by a melt-blending technique using low-density-poly(ethylene) [23].

Continuing our research on laser-induced chemical liquid deposition (e.g. [24–26]), we were interested in exploring the possibility of using UV laser photolysis of Cu(II) acetylacetonate as a clean source of Cu nanoparticles. The conventional lamp photolysis of Cu(II)-1,3-diketonate complexes in alcohols has been reported [27], but neither produced Cu particles, nor the effect of side reactions and additives have been yet elucidated. We now describe that the UV laser photolysis of Cu(II) acetylacetonate in 2-propanol is a simple and clean way for synthesis of Cu/polymer colloids and that aging of these colloids leads to sedimentation of Cu/polymer nanocomposites containing unique amorphous copper phase.

2. Experimental

Samples of Cu(II) acetylacetonate (Aldrich, 30 ml of 1.5×10^{-3} M solutions in 2-propanol (Cica-reagent for spec-

* Corresponding author. Tel.: +420 2 20390308; fax: +420 2 20920661.
** Corresponding author. Tel.: +81 29 861 4550; fax: +81 29 861 4421.
E-mail addresses: pola@icpf.cas.cz (J. Pola), oichi.akihiko@aist.go.jp (A. Ouchi).

1010-6030/$ – see front matter © 2007 Elsevier B.V. All rights reserved.
doi:10.1016/j.jphotochem.2007.05.007

troscopy)) were placed in a quartz tube (3 cm in diameter, 10 cm long) equipped with a valve for connection to a vacuum line. The solutions were de-aerated by using vacuum (three freeze–thaw cycles), bubbled with Ar and irradiated under Ar with an LPX-200 (Lambda Physik) laser. The ArF laser radiation at 193 nm and KrF laser radiation at 248 nm with a repetition frequency of 10 Hz delivering respective energy of 230 and 650 mJ per pulse (measured by a Gentec ED-500 joulmeter) was employed. The solutions were stirred by a magnetic bar and the laser pulses were mildly focused to incident area of 1.2 cm^2 to obtain respective incident fluence of 190 and 540 mJ/cm^2.

The photolytic progress was monitored on the aliquots (0.5 ml) withdrawn from the irradiated solution and diluted with hexane (Cica-reagent for spectroscopy, 3 ml) by UV–vis spectrometry (a Shimadzu UV-2450 UV–vis spectrometer) in the 4 ml quartz cells.

After the photolysis, the solutions were allowed to stay overnight and the black particles precipitated during this period were centrifuged from the solution, washed with hexane, again centrifuged and kept under argon. The centrifuged solutions freed from the particles were analyzed on a Shimadzu QP5050 gas chromatograph–mass spectrometer (60 m long capillary column with Neutrabond-1 as a stationary phase, programmed temperature 30–200 °C). Gases evolved from the irradiated solutions were accumulated in a balloon connected to the quartz tube. The detected photolytic products were identified by using the NIST library.

The effect of additives on the precipitation of the particles was examined by adding small amounts of surfactants (diethylene glycol, polypropylene glycol and poly(methylhydroxysiloxane) (all 0.5 ml)) to the Cu(II) acetylacetonate solutions after the laser photolysis was ceased.

The sediment was analyzed by UV spectroscopy (an UV 1601 Shimadzu spectrophotometer), FTIR spectroscopy (a Nicolet Impact spectrometer), by X-ray diffraction measurements (a PANalytical X'Pert PRO diffractometer equipped with a conventional X-ray tube (Co Kα radiation) and DiffracPlus software package [28]) and by electron microscopy. SEM images were acquired using a Philips XL30 CP scanning electron microscope. TEM analysis (particle size and phase analysis) was carried out on a Philips 201 transmission electron microscope. Process diffraction [29] was used to evaluate and compare measured electron diffraction patterns with an XRD diffraction database [30]. HRTEM micrographs were obtained using a JEOL JEM 3010 operating at 300 kV (LaB6 cathode) and equipped with EDS detector (INCA, Oxford). Nickel grid coated with a holey carbon support film was used. Sediments were dispersed in ethanol and suspension was treated in ultrasonic bath for 10 min.

KrF and ArF-laser-induced photolysis of acetylacetone (Wako) were performed on 2.3×10^{-4} M solutions in hexane (Cica-reagent for spectroscopy).

Diethylene glycol (Wako), polypropylene glycol (Diol Type, 400, Wako) and poly(methylhydroxysiloxane), dimethylsilyl terminated, Aldrich were used as received.

3. Results and discussion

Copper(II) acetylacetonate shows UV absorption spectrum consisting of bands at 280–310, 230–255, and 190–210 nm which are, in the given order, due to a π–π* transition within the ligand, a charge-transfer transition of the ligand-to-metal type, and a blend of π–π* ligand excitation and Rydberg states [31,32]. The chelate shows sufficient absorption in the region of ArF and KrF laser emissions as molar absorptivity at 248 and 193 nm are 1.5 and 4.1×10^4 dm^3 mol^{-1} cm^{-1}, respectively.

3.1. Photolytic features

The laser irradiation at 193 and 248 nm of the Cu(II) acetylacetonate solutions in 2-propanol results in the formation of tiny bubbles observed behind the irradiated quartz wall, development of initially deep brown and later black color of the solution, and deposition of thin shiny films. The bubbles not being observed with the laser irradiation of 2-propanol itself indicate that gaseous products of the Cu(II) acetylacetonate photolysis are expelled from the solution and that the photolysis proceeds just behind the quartz–liquid interface. UV spectral changes in the solutions irradiated with the 193 and 248 nm photons are somewhat different.

The ArF laser photolysis results in a decrease of the Cu(II) acetylacetonate bands at 240 and 290 nm and in a build-up of a new very intense band at 270 nm and weak bands at 420 and 590–600 nm (Fig. 1). The new intense band at 270 nm depleted upon further 30 min irradiation only by ca. 10% (not shown in Fig. 1), indicating that the species displayed by the 270 nm band is upon 193 nm irradiation more stable than Cu(II) acetylacetonate.

The KrF laser photolysis results in a decrease of the Cu(II) acetylacetonate bands at 240 and 290 nm and in a growth of a new medium band at 270 nm, and weak bands at 420 and 590–600 nm (Fig. 2). Conversely to the irradiation with ArF laser, the band at 270 nm becomes significant in neither photolysis stage. This indicates that the 270 nm band species is at 248 nm irradiation less stable than at 193 nm irradiation.

With both 193 and 248 nm irradiations, an intense broad band extends over the whole visible region and it is superimposed on the weak 420 and 590–600 nm bands. The temperature of the ArF laser-photolysed solution remained at 30 °C, whereas that of the KrF laser-photolysed solution increased in several minutes to ∼50 °C. Thin shiny films were deposited at both wavelengths. With 193 nm, the films were mostly deposited on the irradiated area of the quartz wall and were thus detrimental to further photolysis progress. At 248 nm, they covered all surface in contact with the solution and were distinctly seen after the photolysis was ceased and the solution was removed from the tube.

3.2. Assignment of new bands

3.2.1. The 270 nm band

This band has different origin depending on whether photolysis takes place by using ArF or KrF laser. In principle, it can

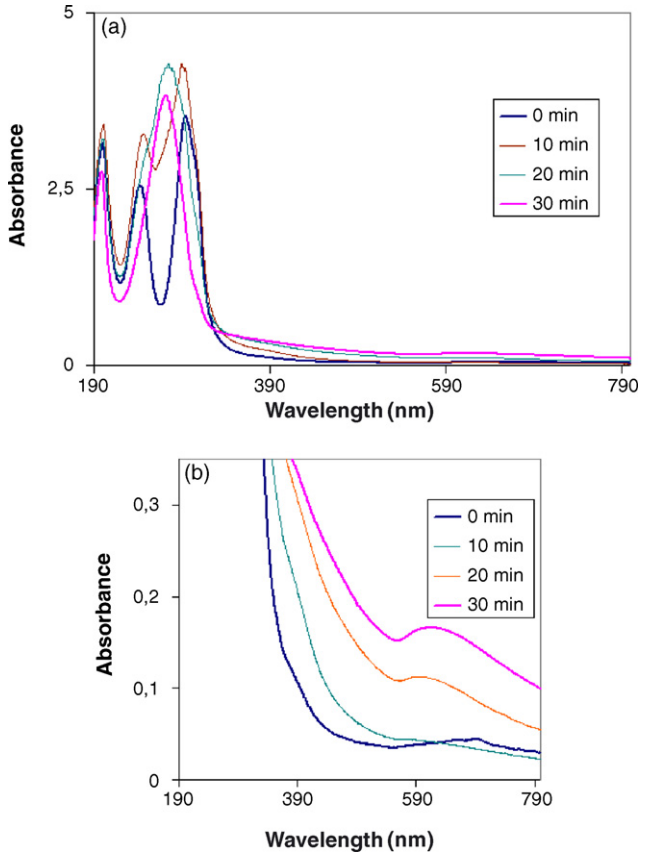

Fig. 1. Absorption spectra of Cu(II) acetylacetonate (1.5×10^{-3} M solutions in 2-propanol) diluted in hexane before and after 10, 20 and 30 min ArF laser irradiation. The total absorbance pattern (a) and enlargement at around 590 nm (b) are given.

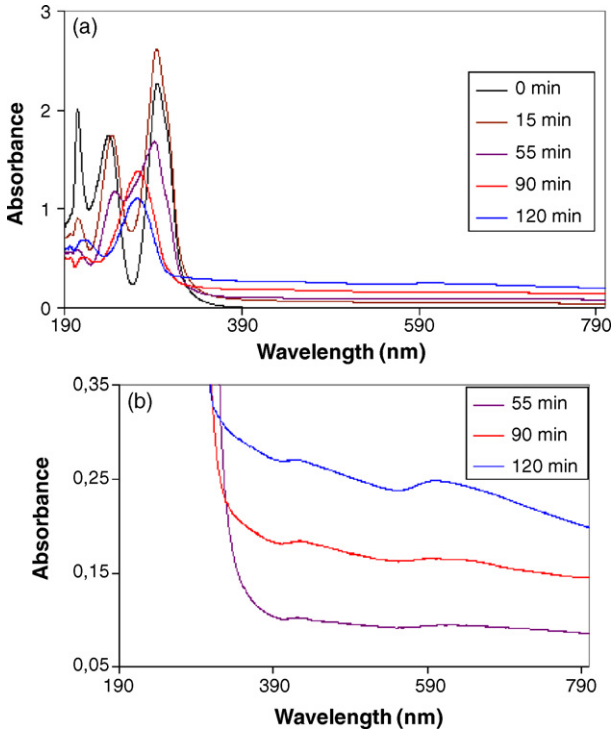

Fig. 2. Absorption spectra of Cu(II) acetylacetonate (1.5×10^{-3} M solutions in 2-propanol) diluted in hexane before and after 15–120 min KrF laser irradiation. The total absorbance pattern (a) and enlargement at around 590 nm (b) are given.

be contributed by a "free" acetylacetone, Cu(I) acetylacetonate and Cu^0 aggregates. Acetylacetone has an absorption at 270 nm (molar absorptivity 9.7×10^4 dm^3 mol^{-1} cm^{-1}) and oligomeric Cu clusters have [10] a band near 300 nm and Cu(I); absorption of acetylacetonate [33], a deduced intermediate [27] in conventional photolysis of Cu(II) acetylacetonate, is unknown.

The nature of the 270 nm band observed with ArF laser photolysis is recognized from the change in the UV spectrum of the ArF laser-irradiated solution staying overnight (Fig. 3). The depletion of this band, the formation of tiny black particles (containing Cu^0, see later) and development of the 230–255 and 280–310 nm bands with absorbance ratio ($A_{(230–255\,nm)}/A_{(280–310\,nm)} = 0.7$) identical to that for Cu(II) acetylacetonate allows unequivocal assignment to Cu(I) acetylacetonate. The observed spectral changes (Fig. 3) can thus be only explained by disproportionation of Cu(I) acetylacetonate (Eq. (1)):

$$2\text{Cu(I)(acac)} = \text{Cu(II)(acac)}_2 + \text{Cu}^0 \quad (1)$$

The 270 nm band observed in the spectra of the Cu(II) acetylacetonate solutions irradiated with KrF laser is, however, of different origin. The band is not only considerably less intense (Fig. 2), but it does not change upon leaving these solutions overnight. This points out that the band has no or negligible contribution from Cu(I) acetylacetonate. Neither has it a significant contribution from acetylacetone that was found as efficiently decomposed by 248 nm radiation (Section 3.3.). These facts assign the band to Cu aggregates.

3.2.2. *The 420 and 590–600 nm bands*

The increase in absorption at 420 nm (related to a shoulder of the 300 nm band) and the weak band at 590–600 nm have been observed [34] for Cu nanosols. The latter band has been assigned (e.g. [10,19,35–37]) to the surface plasmon band of Cu colloids.

The intense broad band extending over the whole visible region and superimposed on both weak 420 and 590–600 nm bands is assigned to light scattering on Cu aggregates.

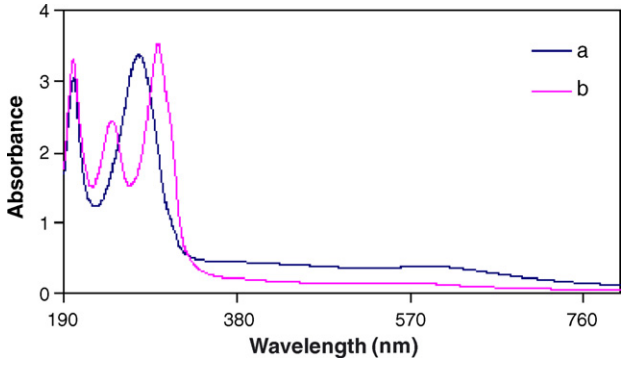

Fig. 3. Spectrum of the solution of Cu(II) acetylacetonate irradiated by ArF laser for 30 min (a) and then left overnight (b).

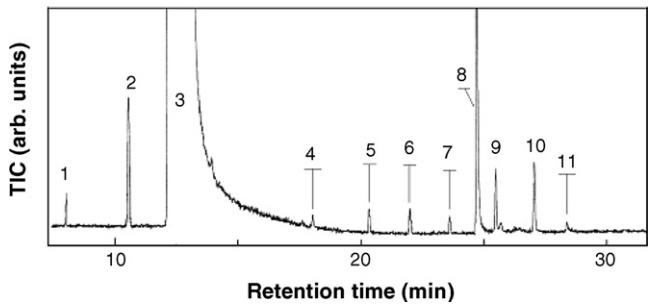

Fig. 4. GC/MS trace of ArF laser-photolyzed solution of Cu(II) acetylacetonate. Designation: (1) acetaldehyde; (2) acetone; (3) 2-propanol; (4) ethenyl acetate; (5) 2-propenyl acetate; (6) 1-methylethyl acetate; (7) ethyl 2-oxo-propanoate; (8) 2,4-acetylacetone; (9) 1-methylethoxy-2-propanol; (10) 2,3-dimethyl-2,3-butanediol; (11) 1,1-dimethylethyl acetate.

3.3. Organic products and photolytic mechanism

Chemical changes monitored in the ArF laser- and KrF laser-irradiated solutions of Cu(II) acetylacetonate by GC/MS involve formation of a multitude of organic compounds (Fig. 4) as ethane, propene, acetaldehyde, acetone, 2,4-acetylacetone and carboxylic acid esters (e.g. ethenyl acetate, 2-propenyl acetate, 1-methylethyl acetate and ethyl 2-oxo-propanoate).

The identification of 2,4-acetylacetone is in keeping with the earlier suggested H-abstraction from the solvent by the ligand radical [27] and the other identified compounds are in line with photolytic decomposition of 2,4-acetylacetone [38] yielding $CH_3^{\bullet}$ and $CH_3CO^{\bullet}$ radicals combining to acetone, and acetone decomposition [39] to CO and ethane.

Independent ArF laser- and KrF laser-induced photolysis of 2×10^{-4} M solutions 2,4-acetylacetone in inert hexane indicates photolytic instability of this compound with respective quantum yields 0.3×10^{-2} and 0.5×10^{-2}. These values compared to corresponding quantum yields of Cu(II) acetylacetonate depletion 7.0×10^{-3} (ArF laser radiation) and 3.3×10^{-4} (KrF laser radiation) reveal that photolysis of 2,4-acetylacetone at both 193 and 248 nm is a faster process than the photolysis of Cu(II) acetylacetonate itself.

Propene is formed from 2-propanol [40]. The observed esters are products of photolytic decomposition of enolic form of 2,4-acetylacetone [41,42] or of reactions of 2,4-acetylacetone photofragments with 2-propanol or propene.

The occurrence of radical species and unsaturated (reactive) photoproducts suggest a multitude of organic reactions leading to formation of higher-molecular oligomers.

The presented spectral changes in the ArF and KrF laser-irradiated solutions are in line Cu(II) acetylacetonate reduction to Cu^0 colloids, which proceeds via intermediate Cu(I) acetylacetonate. The formation of Cu sols thus takes place as a simple and/or twofold cleavage of the ligand radical which abstracts H from alcohol and yields acetylacetonate. The simple cleavage leading to Cu(I) acetylacetonate is evident with ArF laser irradiation. The formation of intermediate Cu(I) acetylacetonate is hidden with KrF laser irradiation, which can be due to more efficient photolytic decomposition of this species at 248 nm or faster disproportionation of this species at higher (∼50 °C) temperature. (We note that the one-photon-induced (Hg lamp) process [27] was explained as a reduction of Cu(II) to Cu(I) acetylacetonate and the disproportionation of the latter species to the edduct and Cu^0.) The steps assumed with the laser photolysis of Cu(II) acetylacetonate are illustrated in Scheme 1.

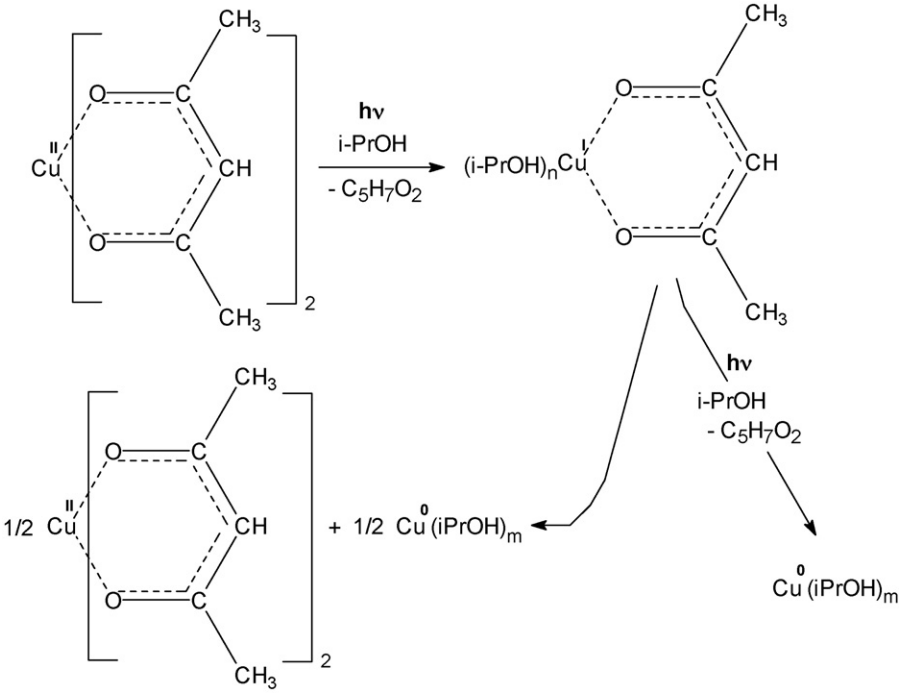

Scheme 1. Decomposition of Cu(II) acetylacetonate.

3.4. Aging of colloidal solutions to sediments

The black solutions of the irradiated Cu(II) acetylacetonate containing Cu sols and Cu aggregates (along with disproportionating Cu(I) acetylacetonate) produce a black sediment and become transparent after staying overnight. The addition of small amounts of diethylene glycol, polypropylene glycol and poly(methylhydroxysiloxane) to the Cu colloidal solutions does not affect the time needed for sedimentation. The stability of Cu colloids in 2-propanol [11,12] is therefore not noticeably improved by addition of these compounds.

However, morphology of the sediments obtained in the absence and presence of additives differs (Fig. 5). Thus, SEM images of the sediments obtained in the absence of additives show rectangular agglomerates composed of discernible bodies, whereas those obtained in the presence of diethylene glycol, polypropylene glycol and poly(methylhydroxysiloxane) reveal irregular, spongy-like structures consisting of merged features.

The EDX-SEM analysis (Table 1) reveals that all the sediments contain copper, substantial amounts of carbon and oxygen and very low amounts of silicon. The amounts of these elements in different sediments are similar.

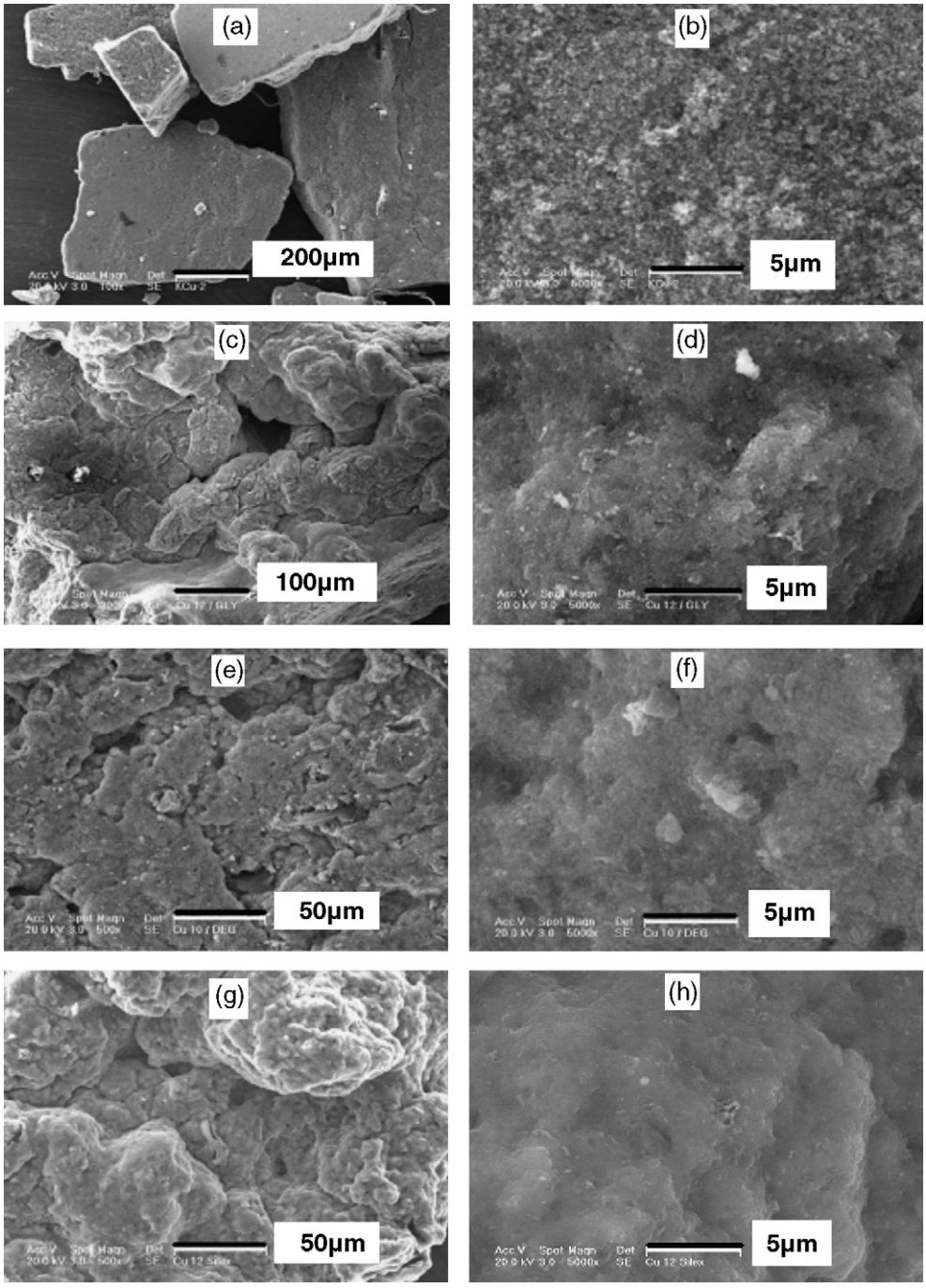

Fig. 5. SEM images of copper-based sediments obtained from ArF laser photolysis of Cu(II) acetylacetonate in 2-propanol in the absence (a and b) and presence of additives (polypropylene glycol (c and d), diethylene glycol (e and f) and poly(methylhydroxysiloxane) (g and h).

Table 1
EDX-derived composition of sediments

Additive	Sediment composition (at.%)			
	Cu	C	O	Si
None	24–33	58–64	8–11	0.5
Diethylene glycol	34–36	28–32	25–27	<1.0
Poly(propylene glycol)	28–30	55–56	14–15	<1.0
Poly(methylhydroxysiloxane)	25–35	49–55	15–17	1.0–1.5

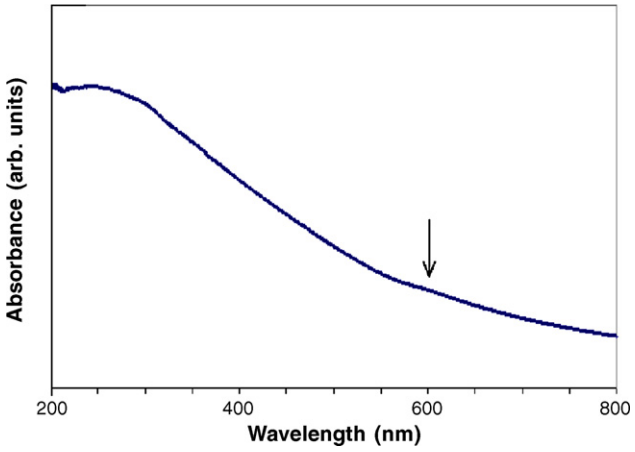

Fig. 6. Typical UV–vis spectrum of the sediment in 2-propanol. The arrow designates a weak band at 600 nm.

These compositions cannot be explained by incorporation of the additives, but are compatible with an incorporation of a high-molecular organic product that cannot be removed in the course of washing of the particles by hexane. Such view gets support from identical UV–vis and FTIR spectra of all the sediments. Typical UV–vis spectrum of the sediments ultrasonically dispersed in 2-propanol shows absorption decaying from 200 nm to higher wavelengths and the very weak but still discernible band at ca. 600 nm (Fig. 6).

Typical FTIR spectrum of the sediment shows absorption bands at 650, 800, 1055, 1260, 1365, 1580, 2850 $2960\,cm^{-1}$ and a broad band with maximum at ca. $3300\,cm^{-1}$ (Fig. 7). Some bands are unequivocally assignable to ν(O–H···O) ($3300\,cm^{-1}$), ν(C–H) (2960 and $2850\,cm^{-1}$), ν(C=C) ($1580\,cm^{-1}$) and ν(C–O) ($1055\,cm^{-1}$) vibrational

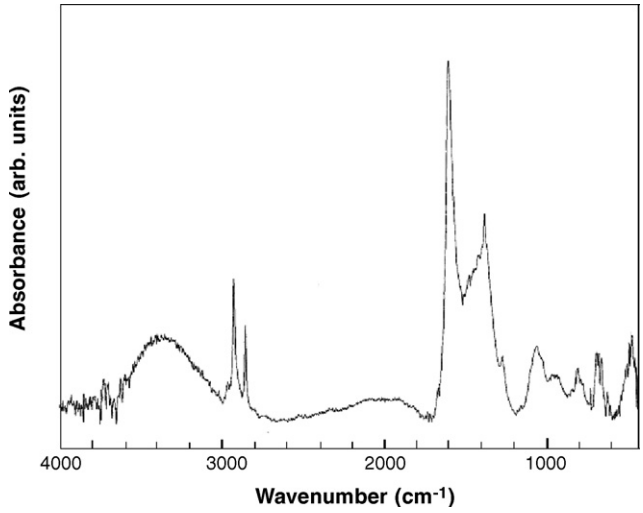

Fig. 7. Typical FTIR spectrum of the sediment film on KBr.

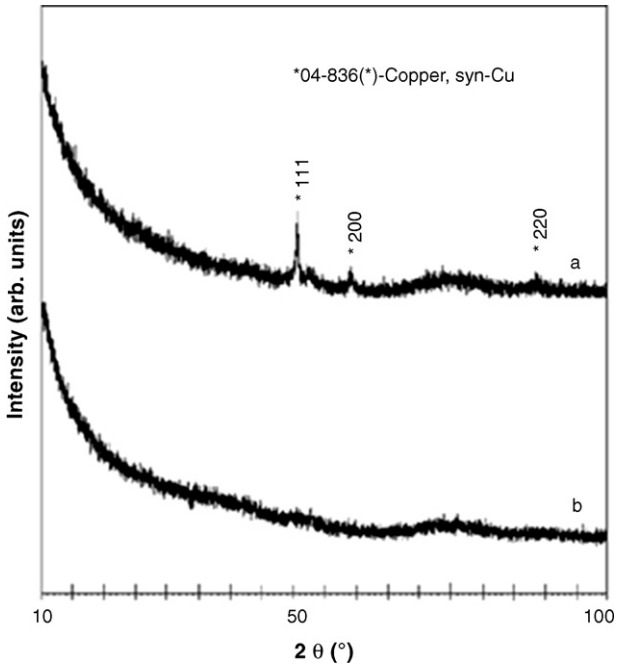

Fig. 8. Powder XRD pattern of the sediment obtained with ArF laser: (a) no additive; (b) polypropylene glycol as additive.

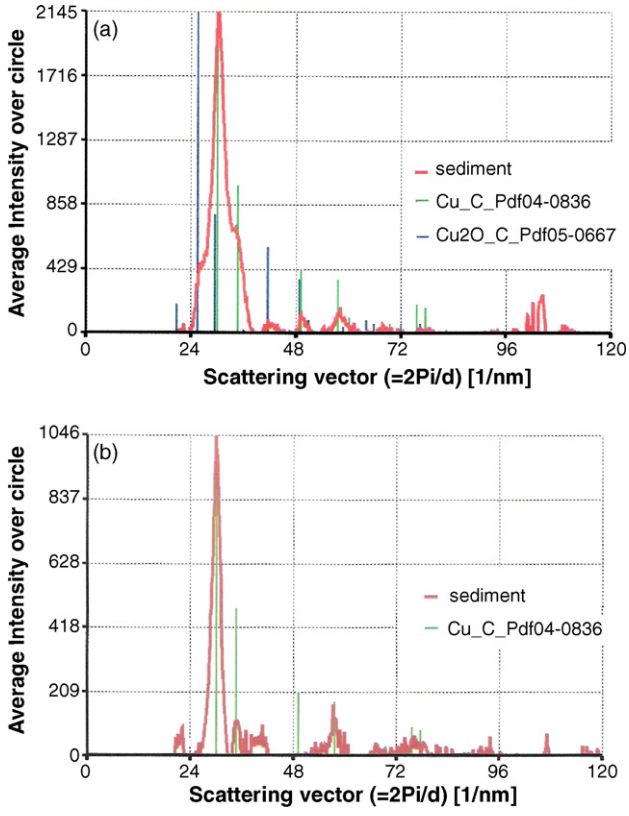

Fig. 9. Electron diffraction pattern of the sediment obtained with ArF laser: (a) no additive; (b) polypropylene glycol as additive.

modes, while others, being of less diagnostic value, correspond to skeletal C/H/O vibrations. The UV spectral features indicate some extent of the C=C bonds conjugation.

These analyses are in line with a photo-polymer produced in the course of laser irradiations by a variety of reactions of radical species and unsaturated photoproducts (Section 3.3) and indicate that the sedimental particles are a blend of elemental Cu and the photo-polymer. Low amounts of silicon (and oxygen) are accountable for by a minor back-side etching of quartz tube (see e.g. [43,44]).

The XRD patterns of the sediments reveal that elemental copper is predominantly in amorphous state. Very rare crystalline features of face centered cubic copper were only revealed by laborious examination of many samples by electron diffraction analysis. Two XRD and electron diffraction patterns are given for illustration in Figs. 8 and 9.

The sediments obtained in the absence of additives typically showed a small contribution of Cu_2O. We speculate that the Cu nanoparticles contained in the solution are not completely covered by the photo-polymer and that the O-containing surface active compounds provide additional protection against feasible oxidation in solution [45]. Such protection may play a role in agglomerization of the nanoparticles during sedimentation process and affect morphology of the sediment.

HRTEM images of the sediments (Figs. 10 and 11) obtained without and with additives do not practically differ and show black, several nm- up to several tens of nm-sized particles embedded in a grayish surrounding. Selective area EDX analysis reveals that the darker bodies are significantly richer in Cu. (Thus, e.g. the stoichiometry of the black bodies and grayish environment in the sediment obtained without additive is $Cu_{1.00}C_{0.90}O_{0.007}$ and $Cu_{1.00}C_{3.95}O_{0.37}$, respectively.)

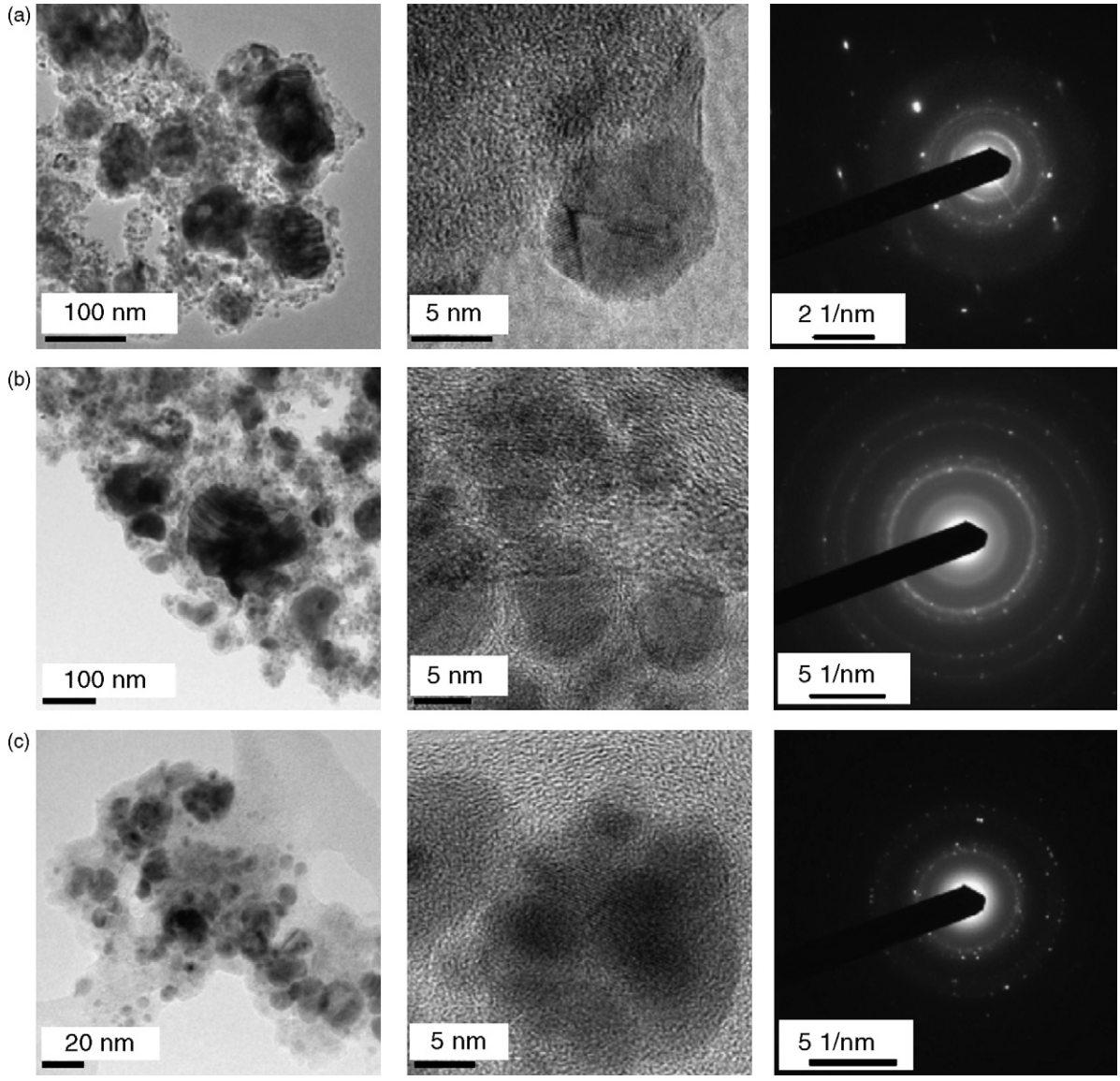

Fig. 10. HRTEM images and selected area electron diffraction (SAED) patterns of sediments obtained without additive (a) and with polypropylene glycol (b) and poly(methylhydroxysiloxane) (c).

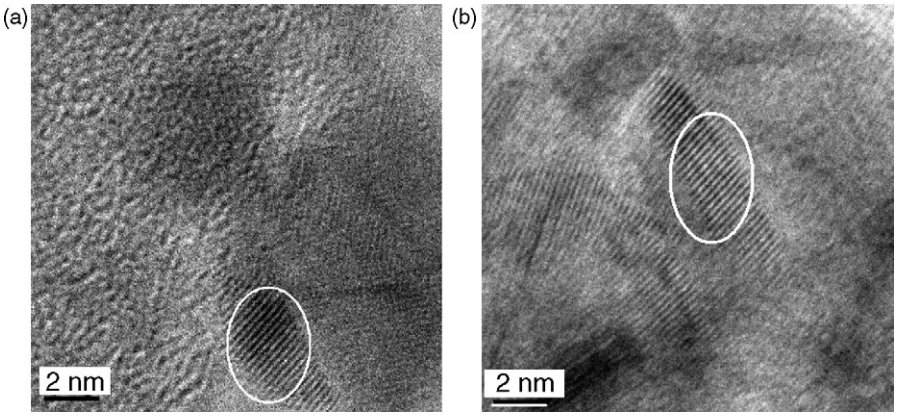

Fig. 11. HRTEM images of the sediment obtained without additive (a) and with polypropylene glycol (b).

The electron diffraction patterns and HRTEM images are also providing evidence on the prevalence of Cu amorphous phase; only few of many images are consistent with a small portion of crystalline Cu (Fig. 11). Fringe spacing of 0.209 nm and interlayed distance of 0.208 nm observed in HRTEM patterns (see Fig. 11a and b) are related to (1 1 1) lattice planes of pure face centered cubic copper (ICDD PDF 04-0836).

We note that the dominating amorphous copper in nanostructured Cu/C/H/O composite represents a rare example of amorphous metal phases. Amorphous copper phase (produced only at ultrahigh pressure [46]) and alloys (e.g. [47,48]) are very rare materials. Formation of amorphous Cu phases is therefore of great interest.

The results of this work reveal an alternative way of production of amorphous copper (and possibly other metals) when embedded in a photo-polymer. The results also contribute to synthesis of Cu/polymer nanocomposites that is under active research (e.g. [23]) as a part of considerable attention given to nanocomposites of metals in polymer matrix.

4. Conclusions

ArF and KrF laser photolysis of Cu(II) acetylacetonate in 2-propanol occurs via intermediate Cu(I) acetylacetonate and yields Cu colloidal solutions in which both Cu nanosols and agglomerates, detected by UV–vis spectroscopy, are embedded in a polymer.

Photolytic formation of the organic polymer is in keeping with many organic photolytic products identified by GC/MS technique, showing a multitude of simultaneously occurring organic reactions.

The aging of Cu colloidal solutions leads to sedimentation of nanosized Cu/polymer agglomerates containing Cu in mostly amorphous phase. Stability of the colloidal solutions is not improved by addition of O-containing surface active compounds, but morphology of the sediments obtained in the absence and presence of these compounds is different.

The presented technique represents a new approach to Cu/polymer nanocomposites (Scheme 2) incorporating very rare amorphous Cu phase.

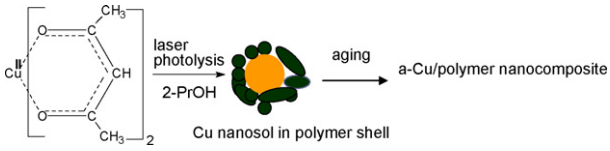

Scheme 2. Formation of Cu/polymer sols and nanocomposite.

Acknowledgement

The authors thank Dr. P. Bezdička for XRD analysis.

References

[1] D.L. Feldheim, A. Foss Jr. (Eds.), Metal Nanoparticles: Synthesis, Characterization and Applications, Marcel Dekker, Inc., New York, 2002.
[2] A. Heilmann, Polymer Films with Embedded Metal Nanoparticles Springer Series in Materials Science, vol. 52, Springer-Verlag, Berlin, 2003.
[3] K.J. Klabunde (Ed.), Nanoscale Materials in Chemistry, Wiley–Interscience, New York, 2001.
[4] X.G. Li, Q.F. Lü, M.R. Huang, Chem. Eur. J. 12 (2006) 1349–1359.
[5] R. Richard, H. Bönnemann, in: C.S.S.R. Kumar, J. Hormes, C. Leuschner (Eds.), Nanofabrication Towards Biomedical Applications, Wiley–VCH Verlag, Weinheim, 2005.
[6] K.L. Kelly, E. Coronado, L.L. Zhao, G.C. Schatz, J. Phys. Chem. B 107 (2003) 668–677.
[7] S. Kapoor, R. Joshi, T. Mukherjee, Chem. Phys. Lett. 354 (2002) 443–448.
[8] S. Kapoor, T. Mukherjee, Chem. Phys. Lett. 370 (2003) 83–87.
[9] S. Kapoor, D.K. Palit, T. Mukherjee, Chem. Phys. Lett. 355 (2002) 383–387.
[10] J. Khatouri, M. Mostafavi, J. Amblard, J. Belloni, Chem. Phys. Lett. 191 (1992) 351–356, and refs. therein.
[11] Y.-H. Yeh, M.-S. Yeh, Y.-P. Lee, C.-S. Yeh, Chem. Lett. (1998) 1183–1184.
[12] M.-S. Yeh, Y.-S. Yang, Y.-P. Lee, Y.-H. Yeh, C.-S. Yeh, J. Phys. Chem. B 103 (1999) 6851–6857.
[13] H.-T. Zhu, C.-Y. Zhang, Y.-S. Yin, J. Cryst. Growth 270 (2004) 722–728.
[14] A.A. Athawale, P.P. Katre, M.B. Majumdar, J. Nanosci. Nanotechnol. 5 (2005) 991–993.
[15] X. Song, S. Sun, W. Zhang, Z. Yin, J. Colloid Interf. Sci. 273 (2004) 463–469.
[16] H. Zhu, G. John, B. Wei, Chem. Phys. Lett. 405 (2005) 49–52.
[17] A.A. Ponce, K.J. Klabunde, J. Mol. Catal. A: Chem. 225 (2005) 1–6, and refs therein.
[18] M.P. Pileni, T. Gulik-Krzywicki, T. Tanori, A. Filankembo, J.C. Dedieu, Langmuir 14 (1998) 7359–7363.
[19] J. Lisiecki, M.P. Pileni, J. Phys. Chem. 99 (1995) 5077–5082.
[20] S.Q. Qiu, J.X. Dong, G.X. Chen, J. Colloid Interf. Sci. 216 (1999) 230–234.

[21] M. Schmittel, V. Kalsani, L. Kienle, Chem. Commun. (2004) 1534–1535.
[22] C.-M. Li, H. Lei, Y.-J. Tang, J.-S. Luo, W. Liu, Z.-M. Chen, Nanotechnology 15 (2004) 1866–1869.
[23] X. Xia, S. Cai, C. Xie, Mater. Chem. Phys. 95 (2006) 122–129, and refs. therein.
[24] J. Pola, J.P. Parsons, R. Taylor, J. Mater. Chem. 2 (1992) 1289–1292.
[25] A. Ouchi, K. Yamamoto, Y. Koga, J. Pola, J. Mater. Chem. 9 (1999) 563–566.
[26] A. Ouchi, T. Tsunoda, Z. Bastl, M. Maryško, V. Vorlíček, J. Boháček, K. Vacek, J. Pola, J. Photochem. Photobiol. A: Chem. 171 (2005) 255–256.
[27] H.D. Gafney, R.L. Lintvedt, J. Am. Chem. Soc. 93 (1971) 1623–1628.
[28] DifractPlus, version 8.0, Bruker AXS, 2002.
[29] J.L. Lábár, in: L. Frank, F. Ciampor (Eds.), Proceedings of EUREM 12 Czechoslovak Society for Electron Microscopy, Brno, Czech Republic, 2000, p. 1379.
[30] Powder Diffraction File, Release PDF-2, International Centre for Diffraction Data, Newton Square, PA, USA, 2000.
[31] J.P. Fackler, F.A. Cotton, W. Barnum, Inorg. Chem. 2 (1963) 97–101.
[32] J.P. Fackler, F.A. Cotton, Inorg. Chem. 2 (1963) 102–106.
[33] R. Nast, R. Mohr, C. Schulze, Chem. Ber. 96 (1963) 2127–2131.
[34] A.A. Athawale, P.P. Katre, M. Kumar, M.B. Majumdar, Mater. Chem. Phys. 91 (2005) 507–512.
[35] K. Kimura, Bull. Chem. Soc. Jpn. 57 (1984) 1683–1684.
[36] I. Lisiecki, M.P. Pileni, J. Am. Chem. Soc. 115 (1993) 3887–3896.
[37] H. Abe, K.P. Charle, B. Tesche, W. Schulze, Chem. Phys. 68 (1982) 137–141.
[38] C.E. McDade, T.M. Lenhardt, K.D. Bayers, J. Photochem. 20 (1982) 1–7.
[39] J. Pola, Y. Koga, A. Ouchi, Tetrahedron 53 (1997) 3757–3766.
[40] J.G. Calvert, J.N. Pitts, Photochemistry, Wiley, New York, 1966.
[41] M.C. Yoon, Y.S. Choi, S.K. Kim, J. Chem. Phys. 110 (1999) 11850–11855.
[42] H.P. Upadhyaya, A. Kumar, P.D. Naik, J. Chem. Phys. 118 (2003) 2590–2598.
[43] J. Wang, H. Niino, A. Yabe, Appl. Phys. A 111 (1999) 111–113.
[44] H. Niino, Y. Kawaguchi, T. Sato, A. Narazaki, T. Gumpenberger, R. Kurosaki, Appl. Surf. Sci. 252 (2006) 4387–4391.
[45] S.-Y. Xie, Z.-J. Ma, C.-F. Wang, S.-C. Lin, Z.-Y. Jiang, R.-B. Huang, L.-S. Zheng, J. Solid State Chem. 177 (2004) 3743–3747, and refs. therein.
[46] H. Furuichi, E. Ito, Y. Kanno, S. Watanabe, T. Katsura, N. Fujii, J. Non-Cryst. Solids 279 (2001) 215–218.
[47] A.H. Brothers, D.C. Dunand, Scripta Mater. 54 (2006) 513–520.
[48] W.H. Wang, C. Dong, C.H. Shek, Mater. Sci. Eng. R 44 (2004) 45–89.